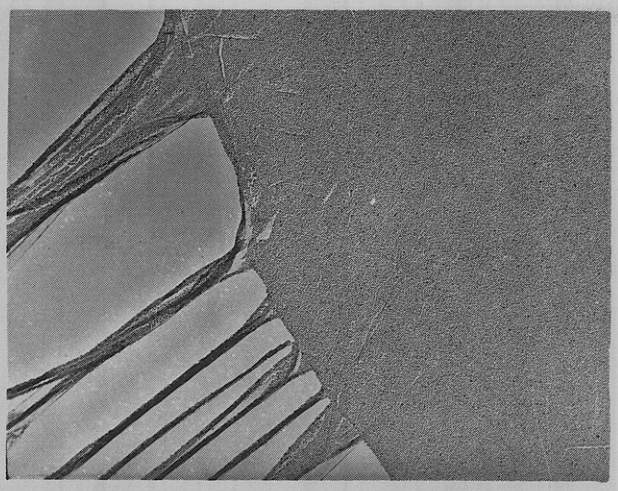

Figure 16. Electron micrograph of large bilayer fibers (magnification 8400×).

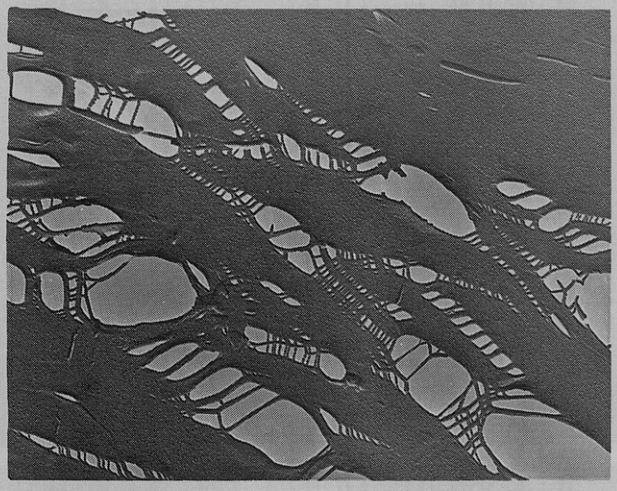

Figure 17. Electron micrograph of small bilayer fibers (magnification 17 500×).

From the birefringence, the presence of the bilayer could be easily seen (Figure 14). In many cases the bilayers have holes which can be seen by lack of birefringence in some areas. Bilayers are fairly stable, especially if kept cold and in the dark. Some bilayers that have been stored on laboratory shelves and exposed to light, however, tend to break in a period ranging from 0.5 to 1 year. This is probably caused by trace amounts of ozone in the air cleaving the polymer backbone over long periods of time.

Electron Microscopy of Bilayers. Bilayers on electron microscope grids were shadowed under a high vacuum with platinum or gold at 45° to enhance any surface features. At low magnification a thin sheet is observed spanning across the grid holes (Figure 15). Small holes are present in some places and may be caused by places in the bilayer where two crystalline boundaries in both layers coincide, resulting in low strength and breakage. The holes may also result from the bombardment of the hot metal particles during the shadowing process. Whatever the origin, films which were made from monolayers containing large crystallites exhibited relatively few holes.

A region where the bilayer has started to break is shown in Figure 16 and exhibits the very fibrous nature of the bilayer membrane. In another region of separation, fibers can be observed from each of the two layers in the bilayer forming a cross-hatched network (Figure 17). The parallel nature of the microfibers is another indication of the unidirectional polymer chain orientation within the monolayer plane in a given crystallite. As would be expected from the crystalline nature, these layers produce highly oriented electron diffraction patterns analogous to single-crystal diffraction. The detailed analysis of this phenomenon is discussed in the following paper.

Acknowledgment. Support of this work under National Science Foundation Grant DMR-77-13001-A01 is gratefully acknowledged.

References and Notes

(1) Day, D. R.; Ringsdorf, H. *J. Polym. Sci., Polym. Lett. Ed.* **1978**, *16*, 205.
(2) Day, D. R.; Ringsdorf, H. *Makromol. Chem.* **1979**, *180*, 1059.
(3) Day, D. R.; Lando, J. B.; Ringsdorf, H. *Polym. Prepr., Am. Chem. Soc., Div. Polym. Chem.* **1978**, *19* (2), 176.
(4) Wegner, G. *Z. Naturforsch.* **1969**, *24b*, 824.
(5) Hartshorne, N. H.; Stuart, A. "Crystals and the Polarizing Microscope"; E. Arnold Ltd.: New York, 1970.
(6) Gay, P. "An Introduction to Crystal Optics"; Longmans, Green and Co.: New York, 1967.
(7) Geil, P. H. "Polymer Single Crystals"; Interscience: New York, 1963.

Structure Determination of a Poly(diacetylene) Monolayer

David Day and J. B. Lando*

Department of Macromolecular Science, Case Institute of Technology, Case Western Reserve University, Cleveland, Ohio 44106. *Received March 11, 1980*

ABSTRACT: Electron diffraction of self-supporting poly(diacetylene) bilayers has shown them to be highly crystalline. Two misregistered diffraction patterns were usually observed, originating from each of the monolayers comprising the bilayer. Weak "superstructural" diffraction intensities and upper layer line smearing were shown to be the result of a systematic type of disorder and were reproduced through laser optical diffraction. The intensities of 13 independent reflections were collected and used to refine the packing within a single monolayer. As a result of the partially ambiguous solution, monomeric monolayer diffraction was used to clarify the packing symmetry and deduce the correct polymer monolayer structure.

Introduction

Recent investigations have indicated the ability of monolayers of certain surface-active diacetylene compounds to undergo polymerization.[1,2] The resulting polymeric monolayer films are rigid and consist of rather large two-dimensional crystalline domains.[3] Two monolayers placed together form self-supporting membranes able to span macroscopic holes.[3] The high degree of order and the thinness of these bilayer films make them suitable for structural investigation by electron diffraction. Due to the high structural integrity of the diacetylene lithium salt monolayers, all discussion in this paper is limited to

0024-9297/80/2213-1483$01.00/0

the following polymer film:

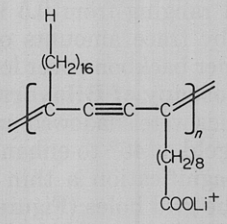

Experimental Section

Monolayers were spread on the water surface and polymerized to completion as shown by visible spectroscopy.[2] Polymer bilayer samples were prepared in the same manner as has been previously described.[3] Bilayer diffraction patterns were obtained with a JEOL JEM 100B electron microscope at 100 kV. Electron diffraction was also obtained from non-self-supporting monomeric monolayers placed on thin carbon films for comparison with the polymeric films. Experimental lattices were produced by computer with varying degrees and intervals of lattice shift to determine the nature of the bilayer packing disorder. The lattices were miniaturized on film and placed directly in a laser optical diffraction apparatus for visual observation.

Results and Discussion

Electron Diffraction of Bilayers. Bilayer diffraction at low beam intensities remained sharp in the electron microscope for as long as 15 s and the inner spots remained for as long as 2 min. A high-speed X-ray film was used in order to record the outer reflections at low beam intensities. With extremely good samples, diffraction intensities could be observed as far out as 0.8 Å. Typically, two diffraction patterns were observed, one arising from each of the monolayers comprising the bilayers (Figure 1, top). The misregistration between the two patterns varied, determined only by the random way in which the layers originally came together. As the sample was scanned, the two patterns were observed to shift as new crystallite orientations passed through the beam (Figure 1, middle). In some cases, regions were found where the two orientations were identical, resulting in a single diffraction pattern (Figure 1, bottom). The unit cell for the structure and indexed spots are given in Figure 2. The *c*-axis repeat distance of 4.9 Å matches the ideal repeat distance of a poly(diacetylene) chain, so it is concluded to be the chain axis. This has been confirmed by the diffraction of a fiber partially pulled between a broken layer. In Figure 3 the *c* axis is observed from the diffraction pattern to lie along the fiber axis, which can safely be assumed to be the chain axis.

In Figure 1, bottom, a distinct smearing of the intensity is observed in the b^* direction and increases with the l index. A possible origin of this may be due to a small disordering in the packing. The type of disorder can be derived from the Fourier transform as being due to a slip in the *c* direction between polymer chains. In some diffraction micrographs where little beam destruction has occurred, the smeared reflections close to the origin are seen to really consist of many distinct spots.

It was first thought that the smearing and spots may be due to a systematic shift distance in the *c* direction occurring at random along *b* or a random shift distance in the *c* direction at systematic intervals along *b* (see Figure 2).

To determine the nature of the disorder experimental lattices were drawn with various kinds of disorder and then placed in a laser optical diffraction apparatus. Through trial and error, optical diffraction patterns very similar to the monolayer diffraction patterns were obtained. The lattice which produced these patterns has a shift in the *c* direction at systematic intervals of about 24 Å along *b*, or three unit cells. This gives the effect of a superstructure and results in the closely spaced spots on the upper layer lines. The shift in the *c* direction must average about 0.8 Å to simulate the correct positions of the low-intensity "superstructure" spots. Although the average shift is 0.8 Å, this must vary from 0.0 to 1.6 Å to produce the observed smearing. The resulting optical diffraction pattern is shown in Figure 4. This closely resembles the monolayer diffraction in Figure 1, bottom, with the exception that, due to the truncated lattice, the smearing is not as great in the simulated pattern.

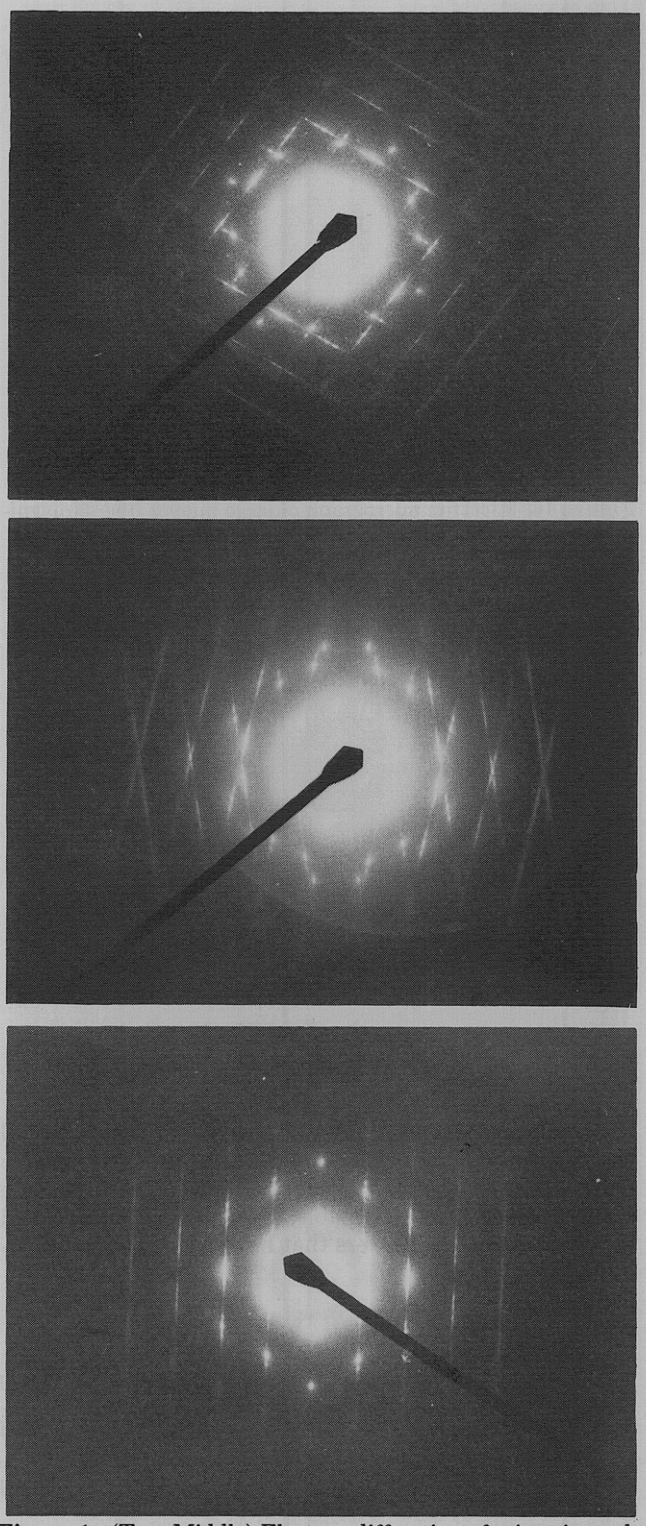

Figure 1. (Top, Middle) Electron diffraction of misregistered layers. (Bottom) Electron diffraction of registered bilayer.

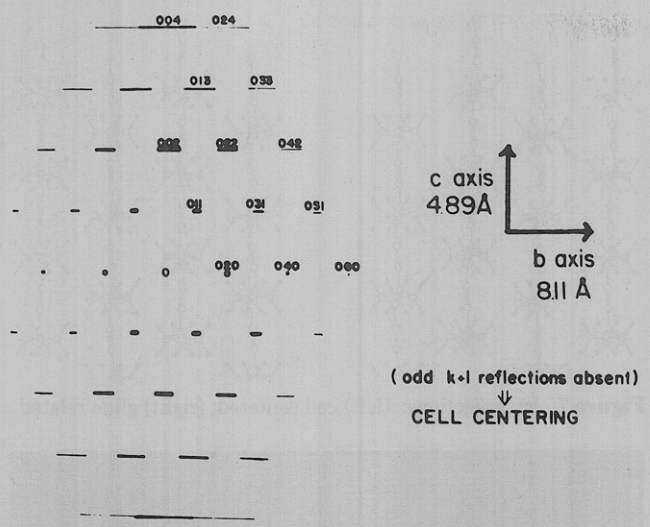

Figure 2. Unit cell and indexing.

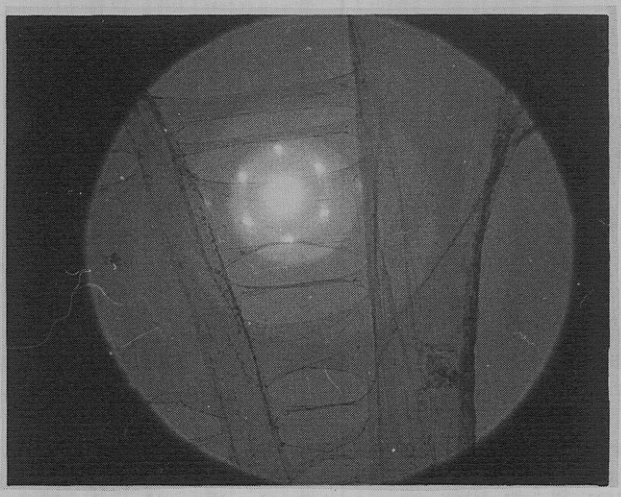

Figure 3. Electron diffraction of separated bilayer (magnification 2310×).

Monolayer Structure Determination. The diffraction pattern in Figure 1, bottom, has 13 independent observable intensities. With these intensities a refinement of the monolayer structure was performed. Despite the 80 atoms per polymer chain repeat unit, major restrictions on the structure reduced the refinement down to one major variable.

The first restriction was that the hydrocarbon side chain must lie perpendicular to the layer plane. This is known from theoretical bond lengths and the thickness measured on multilayers and monolayer fibers.[4] Because a refinement of the projection is being performed, the fact that the hydrocarbon side chains are perpendicular to the plane greatly simplifies the structure by causing a superposition of many of the atoms. All the atoms in the hydrocarbon chain could be represented by a total of 12 properly weighted atoms. Li was excluded for lack of bonding data and its low electron density. Hydrogen atoms were included.

A second restriction lay in the fact that the poly(diacetylene) must lie along what was defined as the c axis as mentioned previously.

The last restriction is that, from the systematic absence of $h + k$ = odd reflections and from the asymmetry of the monolayer, a base centering of the unit cell was known to be present. Since the crystal consists of only one layer, the true symmetry may involve an n glide instead of an A centering. X-ray diffraction data indicate a doubled

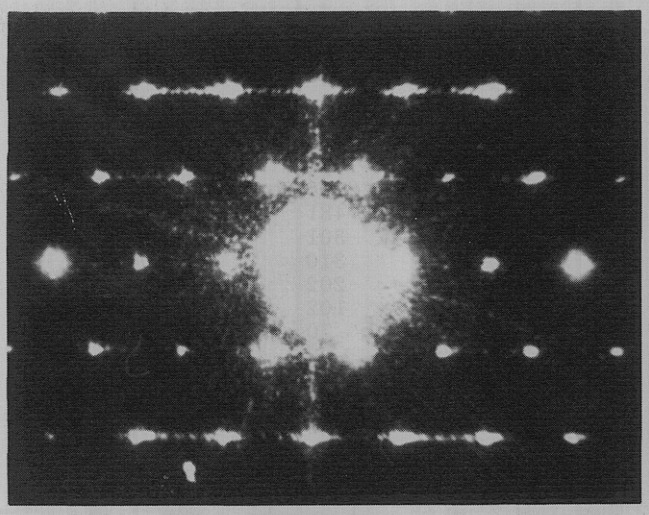

Figure 4. Laser optical diffraction pattern from simulated defect structure.

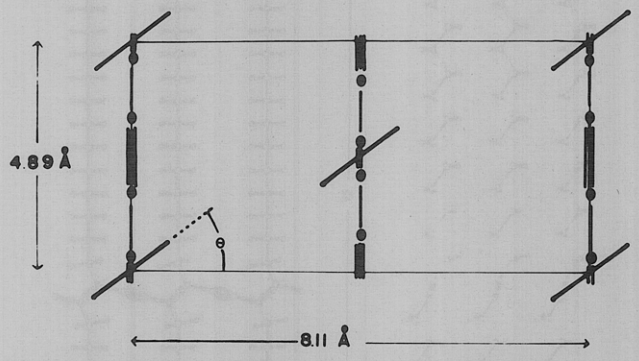

Figure 5. Polymer monolayer structure schematic.

repeat in the a direction. Thus we are dealing with half the unit cell in the a direction.

With these restrictions a schematic diagram of the unit cell can be drawn where most of the structural information is known before any refinement (Figure 5). The schematic shows the backbone along the c axis, a cell centering and diagonal lines representing the superimposed planar zigzag of the hydrocarbon side chains. The major structural aspect that is not known is θ, or the angle between the b axis and the planar zigzag.

Intensity data were digitally collected from a series of three electron microscope diffraction negatives on a Photometrics densitometer and intensity printouts were obtained.

The intensities were numerically summed and the backgrounds subtracted. The 033, 024, and 002 reflections were used to scale the intensities of the three films into a final set of structure factors.

Calculated structure factors were obtained for a series of models, using standard bond lengths and angles with θ (Figure 5) ranging from 0 to 90°.

Electron scattering factors were used in the calculation[5] and, because hydrogen has a much higher scattering factor with respect to carbon in electron diffraction in X-ray diffraction, hydrogens were included in the refinement. Although dynamic diffraction is an effect which normally arises from "rediffraction" of diffracted electrons, this was not a factor in the bilayer samples due to their thickness of only two half-unit cells and the clear absence of $k + l$ odd reflections.

In the structure refinement, a distinct minimum in the residual,[6] where

$$R = [\Sigma||F_o| - |F_c||]/\Sigma|F_o|$$

Table I
Comparison of Observed and Calculated Intensities for the Model in Figure 7 (Left)

hkl	F_o^2	F_c^2
011	12000	12187
020	7011	6367
002	2406	2824
022	481	1079
031	301	264
013	310	372
004	202	114
040	102	67
024	70	23
033	93	107
042	30	32
051	25	16
060	10	11

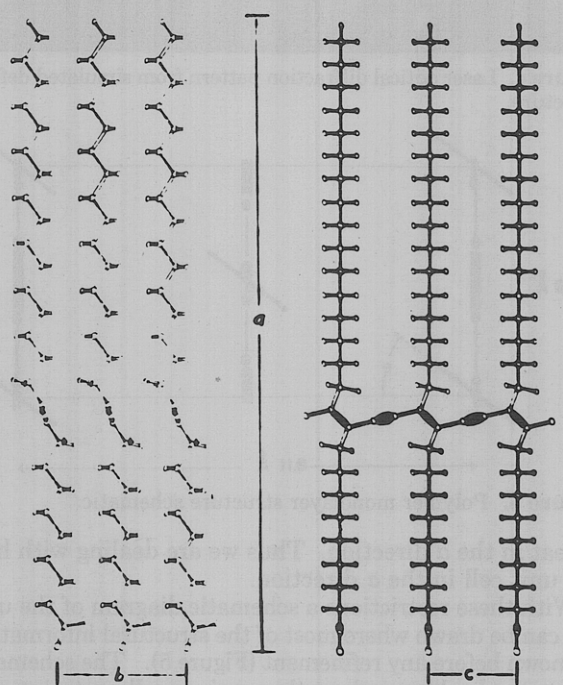

Figure 6. Polymer monolayer structure.

was found at 0° in θ. This was found to agree well with the Patterson map (resulting from a Fourier synthesis performed with the intensities and indicating major interatomic bond vectors[7]), where only two major peaks are discernible and correspond in angle and length to the carbon–carbon and carbon–hydrogen bond vectors.

The final residual has a value of 9%, which is unusually low for such a refinement, but upon inspection of the observed and calculated structure factors (Table I) it is seen that the residual is heavily weighted by the agreement of the first three or four reflections. There are some substantial differences in some of the lower intensities but, overall, the agreement is fairly good. It is thought that the differences are caused by error in measurement, the remains of monomer trapped in the polymer layer, or the fact that no correction for the lattice disorder was made (smeared spots were integrated as one intensity).

Monolayer Structure. The final monolayer structure is shown in Figure 6. The actual *bc* projection that was refined is shown in Figure 7, left, with the acid end group omitted for clarity. The hydrocarbon tails on each side of the diacetylene backbone do not superimpose, causing two planar zigzags for each repeat unit.

The solution was found to be nonunique, however, in that a slight variation gave the same residual of 9%. This variation has a glide plane along *b*, violating the cell centering mentioned earlier, but it is so similar to the first model that the absent reflections remain absent. The only difference in the structure is in the diacetylene backbone itself (Figure 7, right), while the position of the hydrocarbon side chains remains the same. The residual does not change significantly because the carbons in the backbone make up only about 11% of the total electron density in the monolayer and the atomic positions in the *bc* projection vary less than 0.5 Å. The determination of which of the two models is correct depends on the structure of the initial monomer monolayer.

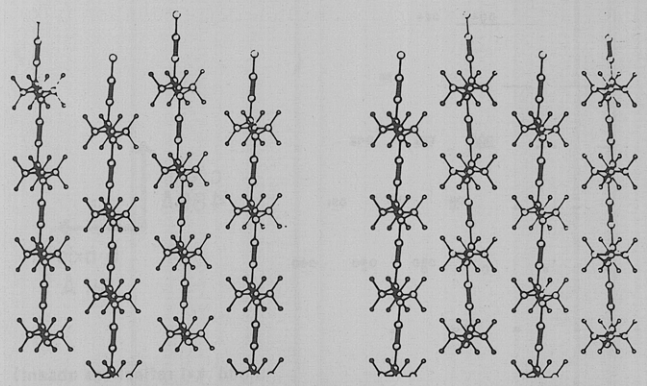

Figure 7. *bc* projections: (left) cell centered; (right) glide related.

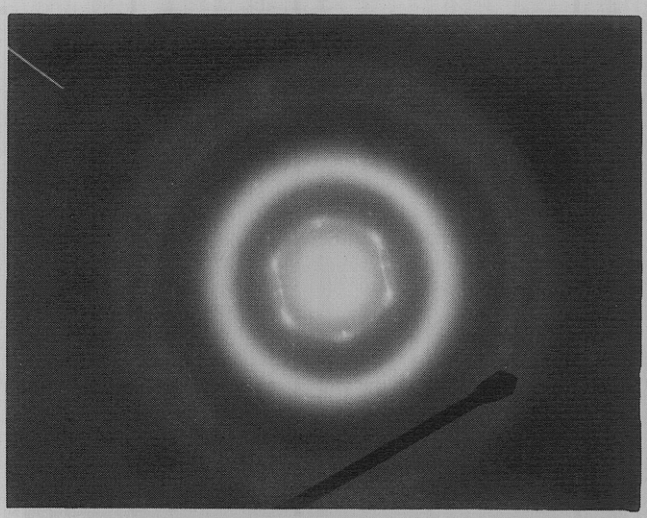

Figure 8. Monomer monolayer diffraction.

Monomer Monolayer Diffraction. Diffraction of monomeric monolayers was obtained by depositing single monomeric films onto electron microscope grids which had been previously coated with a thin carbon film. The carbon film acted as a support for the non-self-supporting monomer monolayers. The diffraction patterns (Figure 8) reveal an orthorhombic lattice net, where b = 9.2 Å and c = 4.83 Å. The area decrease from the monomeric unit cell (44.4 Å^2) to the polymeric cell (39.6 Å^2) corresponds to an 11% contraction and agrees very well with the contraction observed during polymerization under constant pressure.[1]

The monomer diffraction pattern has a systematic absence (0k0, odd reflections absent) which can be due to either a screw axis or a glide plane. The possibility of a screw axis can be eliminated from the fact that a single monolayer is being dealt with and all the hydrophilic heads are on one side of the monolayer. The resulting glide plane along *b* and perpendicular to *c* is consistent with an orthorhombic polyethylene-like projection.

Comparison of Polymer and Monomer Structure. In contrast to the polymeric monolayer, the monomer

hydrocarbon side chains are not perpendicular to the monolayer plane. This is known from 62-Å d spacing obtained from X-ray diffraction of built-up monomeric Li salt bilayers (multilayers). From the theoretical monomer bilayer thickness of 74 Å, a tilt angle of 57° is obtained (57° between the monolayer plane and the hydrocarbon axis). In considering a reasonable structure for the monomer, it can be assumed that the axes of the hydrocarbon side chains are parallel to one another (as in all forms of polyethylene[8] and low molecular weight paraffins[9]) for energetic reasons. To have all the hydrocarbon axes parallel and preserve the glide-plane symmetry along b, the tilt of the chains (with respect to the monolayer plane) must be toward the b axis (making c a unique axis).

As indicated by optical microscopy, the θ value (the angle between the planar zigzag and the b axis) is probably on the order of 50°.[3]

A monomeric structure with a tilt angle of 57° toward b and a 50° value of θ could only polymerize to the polymer structure as indicated below, where only the diacetylene rods and planar zigzags are represented.

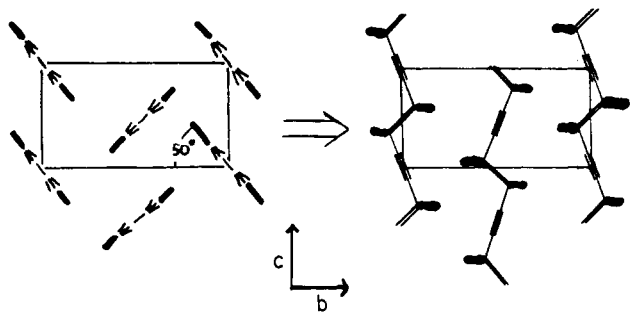

The resulting polymer has a glide-plane symmetry along b which is identical with that in Figure 7, right, and is a good indication that this is the actual polymer structure.

Conclusions

The results presented in this paper, when taken together with those previously reported,[1-3] clearly indicate that the polymerization reaction proceeds in the monomer phase indicated above. A phase change from the monomer structure to the glide-related polymer structure occurs after appreciable conversion.

Acknowledgment. Support of this work under National Science Foundation Grant DMR-77-13001-A01 is gratefully acknowledged.

References and Notes

(1) Day, D. R.; Ringsdorf, H. *J. Polym. Sci., Polym. Lett. Ed.* **1978**, *16*, 205.
(2) Day, D. R.; Ringsdorf, H. *Makromol. Chem.* **1979**, *180*, 1059.
(3) Day, D. R.; Lando, J. B. *Macromolecules*, preceding paper in this issue.
(4) Day, D. R.; Lando, J. B., submitted to *J. Polym. Sci., Polym. Phys. Ed.*
(5) Doyle, P. A.; Turner, P. S. *Acta Crystallogr., Sect. A* **1968**, *24*, 390.
(6) Stout, G.; Jenson, L. "X-Ray Structure Determination"; Macmillian: New York, 1968.
(7) Woolfson, M. N. "X-Ray Crystallography"; Cambridge University Press: New York, 1970.
(8) Yemni, T.; McCullough, R. L. *J. Polym. Sci., Polym. Phys. Ed.* **1973**, *11*, 1385.
(9) Kitaigordoskii, A. I. *Sov. Phys.—Crystallogr.* **1957**, *2*, 454.

Copolymer Structure through Charge Injection and X-ray Photoemission

T. J. Fabish* and H. R. Thomas

Xerox Corporation, Rochester, New York 14644. *Received January 21, 1980*

ABSTRACT: X-ray photoemission and contact-charge injection experiments are applied to random styrene/methyl methacrylate and random and block styrene/2-vinylpyridine copolymer systems as well as to the homopolymers to investigate the electronic structures of the copolymers. The lowest energy electronic excitations and the observable polymer charge state distributions are governed by the electronic structures of the phenyl, ester, and pyridine pendent groups in these polymers, and their individual responses are easily discernible experimentally. Hence, preservation of the characteristic pendent-group responses in the random Sty/MM copolymer indicates that an insignificant perturbation occurs in the constituent moieties at a molecular level and for all copolymer molar ratios. This is not the case for random Sty/2VP wherein a strong pendent-group interaction takes place which significantly alters features of the XPS spectrum and the copolymer charge-state distribution. The thermodynamic drive for the interaction is discussed in terms of chemical potential values deduced from the homopolymer charge-state distributions. In contrast, the block Sty/2VP copolymer exhibits superposition of the characteristic constituent responses similarly to random Sty/MM. However, superposition occurs in this case because the thermodynamically favored pendent-group interaction is limited in extent by the formation of essentially homopolymer domains in this incompatible block system. The electronic response of the block Sty/2VP copolymer is observed to exhibit a pronounced dependence on the thermal history of the film, and rather persistent solvent effects may be present. These results emphasize the importance of electronic interactions, geometrical constraints, and film-forming technique in determining the electronic properties (and surface composition) of copolymers.

Introduction

Recent experimental[1,2] and theoretical[3-7] investigations of saturated carbon chain polymers have shown how large pendent groups can provide localization sites (charge states) for excess charge carriers in the solid created, say, upon carrier injection during contact with another material or by ejection of an electron in a photon-assisted emission event. Moreover, large pendent groups tend to dominate the lowest energy neutral (excitonic) electronic excitations[5-7] as well as those associated with charge states. The prominence of the pendent groups in neutral and charged excitation processes occurs because the molecular orbitals

* Present address: Ashland Chemical Company, Columbus, Ohio 43216.

0024-9297/80/2213-1487$01.00/0